Hybrid Monte Carlo - Particle-in-Cell Simulation of an Ion Thruster Plume

Douglas B. VanGilder*, Gabriel I. Font†
and Iain D. Boyd‡
Cornell University, Ithaca, NY 14853, U.S.A.

Abstract

A numerical code is described that simulates the plumes of electric propulsion engines including ion thrusters and stationary plasma thrusters. In the present study, computed flow field results are compared to existing experimental measurements for the UK-10 ion thruster. The experimental measurements consist of ion flux, ion density, and floating potential data. The numerical code combines the direct simulation Monte Carlo method for modeling collisions with the Particle-in-Cell method for modeling plasma dynamics. Xenon neutrals and ions are modeled directly using particles. Electrons are described by the Boltzmann relation. The effect of a finite back pressure experienced in laboratory experiments is included. Agreement between simulation and experiment is satisfactory. The simulation results are found to be very sensitive to input conditions assumed at the thruster exit plane. In particular, there is uncertainty in specifying the effects of the curvature of the dished grids of the UK-10 thruster on the ion exit velocity profile.

Introduction

It is necessary to understand the plumes of spacecraft propulsion systems for assessment of spacecraft impingement and contamination issues. For ion thrusters and stationary plasma thrusters (SPT), of particular concern are the plume divergence angle for impingement, and charge exchange plasma for contamination by heavy metallic ions. In these devices, not all of the atoms are ionized before exiting the thruster. Therefore, neutrals close to the thruster that have thermal velocities may collide with ions. Some of these collisions lead to charge exchange reactions in which an electron is transferred from the neutral to the ion. This process forms highly energetic neutrals and ions with thermal speeds. These slow ions may interact with conducting surfaces on the spacecraft possibly altering the surface properties. On ion thrusters, they may be pulled back by the potential grids causing grid erosion. The charge exchange plasma leads to spreading of the beam and to acceleration of heavy metallic ions into the plume backflow region. The behavior of charge exchange ions is therefore of particular interest.

A hybrid direct simulation Monte Carlo[1], Particle-in-Cell[2] (DSMC-PIC) code is being developed to understand in detail the plasma behavior of the plumes of ion thrusters and SPT's. The PIC method determines the trajectories of charged particles as predicted by imposed and self-consistent electric fields. The DSMC method is used to deal with the collisional effects in the flow field. Both charge exchange and momentum transfer collisions are modeled. The code is tested on the UK-10 thruster using xenon as a propellant, because of the availability of experimental data. The UK-10 is an electron bombardment ion thruster with a 10 centimeter nozzle exit diameter.[3] The simulation results are compared to measurements of ion flux and floating potential by de Boer,[4] and to measurements of ion density obtained by Pollard.[5]

Numerical Method

There are several issues that need to be addressed to simulate the plumes of ion thrusters. Computational grids must be generated based on disparate length scales that describe the plasma and collision phenomena. Appropriate boundary conditions for the electric field must be imposed. The behavior of the charge exchange ions is determined by the beam ions, the neutrals, and the electric and magnetic fields. The following subsections describe the important aspects of the present implementation.

*Research Assistant.
†Post-Doctoral Research Associate.
‡Associate Professor.

Copyright ©1997 by the Electric Rocket Propulsion Society. All rights reserved.

Neutrals

Earlier work by Roy et al.[7] employed only the PIC method to model ion thruster plumes. The spatial distribution of neutral atoms was specified through an analytical expression. A source term was then used for the charge exchange ions based on an analytical production rate. The current DSMC-PIC code tracks the neutrals (and their properties) as well as the ions. Charge exchange ions are generated directly from collisions between neutral atoms and ions. The probability of charge exchange is based on the relative velocity through collision cross-section given by Rapp and Francis.[6] Propellant utilization efficiencies for ion thrusters are generally well above 50%. Due to their very low velocities, however, the density of the neutrals is higher than the ion density at the thruster exit. Therefore, the behavior of these neutrals determines the rate and location of the charge exchange reactions. Sonic conditions for the neutrals are assumed at the thruster exit based on a stagnation temperature of 500 K. An accompanying paper[8] demonstrates that the assumption of sonic flow agrees well with experiments of neutral xenon flows.

Background Gas

Ground-based experiments have a finite background pressure determined by the capacity of the pumping system. Although this usually gives a density well below the exit density of the neutrals, the two values become comparable in the near plume. Thus, the background density must be included in the simulations. It is assumed to be composed entirely of xenon neutrals, because the beam ions are moving at much higher velocities and thus leave the domain more easily. These neutrals collide with ions and neutrals which originate from the thruster. The background particles are not simulated directly, because it is not necessary to update their positions or know their exact properties. Instead, in each computational cell, temporary particles are created with velocities sampled from a Maxwellian distribution at 295 K. The background density is assumed to be uniform. This is reasonable away from the thruster where its effects are as significant as the foreground neutrals. It is not necessary to model collisions between pairs of background atoms. It is assumed that the background distribution is unchanged with collisions. This assumption is reasonable, since the largest change would be due to the fast atoms created through charge exchange. The magnitude of their density is about three orders of magnitude below the total background density for the case under consideration.

Charged particles

The PIC algorithm uses charged particles and determines the charge density at the nodes of the grid cell based on the proximity of each particle to the surrounding nodes. The scheme developed by Ruyten[9] has been shown to conserve charge density as well as charge. The charge density is then used to calculate the potential at the nodes. Quasi-neutrality ($n_i \approx n_e$) is imposed in the simulation allowing the self-consistent potential field to be determined by the Boltzmann relationship:

$$n_i = n_{ref} \exp\left[\frac{e\phi}{kT_e}\right],$$

where n_i and n_e are the ion and electron densities respectively, e is the electron charge, ϕ is the potential, k is the Boltzmann constant, and T_e is the electron temperature. This is valid for a collisionless, isothermal plasma where the gradients in potential are due to gradients in density and magnetic field effects are negligible. Since magnetic forces of ion thrusters are small compared to electrostatic forces, their effects are ignored.

To find the potential, a value for the electron temperature is required. Experimental work with xenon ion thrusters[4] gives a value ranging from 0.5 to 3.0 eV depending on where in the flow field it is measured. A value of 1.0 eV is chosen for most of these simulations and is compared to a test case with $T_e = 5.0\ eV$. The ratio of collision frequency to plasma frequency ($\frac{\nu}{\omega} \approx \frac{ln N_D}{N_D}$), where N_D is the number of charged particles in a Debye cube, is used to gauge collisionality. This ratio ranges from 1.7×10^{-3} for $1.0\ eV$ to 1.9×10^{-4} for $5.0\ eV$ based on the average ion density at the thruster exit. Since these values are much less than one, it is reasonable to consider the plasma to be collisionless.

The difference in magnitudes of the ion and electron velocities makes it difficult to include the electrons in the simulation. By assuming that the plasma is quasi-neutral, the ion density can be used to find the potential, and the electrons need not be simulated. The ions are assumed to be singly charged, although the code is capable of handling multiple-charged ions.

Grids

The length scale for which a plasma can be treated on a molecular level is given by the Debye length. This length is generally used to scale the computational grid cells in PIC simulations. Grid cells used

for DSMC are generally scaled by the mean free path, the length scale for collisions. Both lengths are functions of density. For the properties of ion thrusters, the Debye length is usually much smaller than the mean free path. Therefore, two different grids are employed by the code. There is no interaction between the two grids. The underlying DSMC code (MONACO[10]) is capable of handling unstructured grids, while the PIC part of the code uses non-uniform regular grids. Memory may become an issue with two grids modeling a large domain. Therefore the PIC grid is implemented implicitly. The only values necessary for each node of the cells are its potential and its electric field vector. The positions of the nodes are stored implicitly in two one-dimensional arrays, rather than in a two-dimensional array. This modification does not affect the computational time significantly, but can save a significant amount of memory.

Boundary conditions

The exit plane of the ion thruster has a physically imposed boundary condition given by the potential of the accelerating grid. The nodes of the PIC grid that lie on the exit plane of the thruster have a potential given by the sum of the accelerator grid's potential and the contribution of the nearby ions. The wall of the thruster is assumed to be biased to the spacecraft potential which is estimated to be kT_e/e.[7] The reference density defined at a location where the potential is set to zero (n_{ref}) is needed for the Boltzmann relationship to obtain the potential. This value is obtained by matching the ion density at the thruster exit nearest the axis with an extrapolation of the potential measurements taken along the axis by de Boer.[4]

Experimental results of ion thrusters suggest a Gaussian distribution of current density.[4,12] Therefore the Gaussian ion density profile assumed by Wang et al.[11] is used at the exit plane. The UK-10 ion thruster has both the screen grid and the accelerating grid dished inward to provide mechanical stability and to reduce beam divergence.[3] The effect of this curvature on the exit profile of the ions is unknown, and its effect on the atoms is assumed to be negligible. By using a dishing depth of 5 mm, various exit profiles are tested.

The domain is assumed to be axisymmetric about the thruster centerline. The main three dimensional effects would come from the location of the neutralizer, but the quasi-neutrality assumption makes these effects negligible. The radial electric field is set to zero on the centerline to satisfy symmetry, but axial variations in potential are permitted. The upper boundary also allows only axial variations in potential. The other two boundaries allow radial but not axial variations in potential. This assumption is valid when the domain is sufficiently large. Particles which reach boundaries other than the symmetry line leave the simulation.

Integration of the two particle methods

The DSMC and PIC methods are compatible because they require very little interaction. The collisions are handled by the DSMC algorithms as are the updating of particle positions and the output of macroscopic variables. The PIC algorithms determine the electric field vector from the potentials at the nodes. The change in particle velocities due to this electric field is then combined with changes due to any collision to update the velocities and then positions. The initial properties of the particles are based on a specified distribution function.

The main incompatibility is due to scale length discrepancies. As mentioned earlier, two separate grids can be easily maintained. This leads to two problems. First, for reasonable statistics, the PIC method needs about 10 ions per cell. This leads to using a larger number of particles per DSMC cell than is usually needed. Over 1,000 particles, including atoms, are used in some cells. The other issue is the time scale. For both methods it is desirable to have a particle remain in a cell for a few time steps. Fortunately, the gradients in ion density in the axial direction are less pronounced than in the radial direction and the ions are moving predominantly in the axial direction. This allows larger axial PIC cell lengths, so that the time scales for the two methods agree. The time scale of choice is the inverse of the ion plasma frequency, the frequency at which the ions oscillate about their equilibrium positions.

Results and Discussion

The conditions specified for the simulations are flow rate ($\dot{m} = 0.73\ mg/s$), thrust (18 mN), beam current (0.33 A), and beam voltage (1,100 V). The back pressure in the vacuum tank is assumed to be 2×10^{-6} torr. The computational domain is comprised of 1,400 DSMC cells and 3,900 PIC cells. It extends 1.3 m axially and 0.70 m radially from the thruster exit. The nodes of the DSMC cells in the ion beam lie on nodes of the PIC grid in this region. The execution time is about 48 hours for a 500,000 particle simulation on an R10000 SGI workstation.

The aforementioned Gaussian density profile is

combined with a constant ion velocity of 40 km/s at the exit, as predicted by a voltage drop of 1100 V. This case is used as a starting point to test the behavior of the code. Figure 1 shows the ion flux versus radial position at various axial locations. The profile is maintained throughout the region, but the magnitude at the centerline decreases along the axis, as the beam spreads. Figure 2 shows the results from the same inlet profile at an electron temperature of 5.0 eV. Comparing the two shows that the ion temperature is not the only cause of spreading. The potential gradients are magnified by a larger electron temperature for similar density gradients.

These results are not surprising if one considers the magnitude of the electrostatic forces compared to the hydrodynamic forces. As the ion beam passes through a cell in the computational domain, it experiences an electrostatic force in the radial direction, since the gradients in density are steepest in that direction. The ratio of this to the axially directed force should give a measure of the amount of spreading of the beam across a cell. The electrostatic force across a cell is:

$$F_E = NqE = Nq\frac{\Delta\phi}{\Delta y}$$

where $\Delta\phi$ is the change in potential and Δy is the radial grid node spacing. Here N is the number of ions in the volume represented by the cell, q is the charge of an ion (+e), and E is the electric field magnitude. The hydrodynamic force is:

$$F_{mv} = \dot{m}u_x = \rho u A u = \bar{n}mu_x^2 A$$

where $\dot{m}$ is the flow rate and u_x is the axial velocity. The area A is of the cell face, ρ is the mass density, $\bar{n}$ is the average ion number density, and m is the mass of an ion. The ratio of the two is given by:

$$\frac{F_E}{F_{mv}} = \frac{Nq\Delta\phi}{\bar{n}mu_x^2 A\Delta y} = \frac{q\Delta\phi}{mu_x^2\frac{\Delta y}{\Delta x}}.$$

Since q and m are known and assuming $u_x \approx$ 35 km/s due to deceleration close to the grid, this gives a value of $6 \times 10^{-4}\ \frac{\Delta\phi}{\Delta y/\Delta x}$. This indicates that the bending of the beam is only significant for large changes in potential across the cell. Using the Boltzmann relationship, the change in potential varies as $T_e ln(\frac{n_2}{n_1})$, where n_1 is the ion density at the lower node and n_2 is the ion density at the upper node. Inside the beam this density ratio is between 1 and 5 which would not make a very significant potential difference. With a higher electron temperature, the spreading is more pronounced as shown in Figure 2.

The constant velocity case is run with and without back pressure. Figure 3 shows the contours of the density of the charge exchange ions for the two cases. In both cases, it is clear that their production is significant. Ions spread due to electric fields. These forces are strongest on the edge of the beam where density gradients are largest. The beam ions are moving so quickly in the axial direction that they are not affected as much as the charge exchange ions. The electrostatic forces pull these charge exchange ions away from the beam. This is most apparent near the thruster exit where most of the charge exchanges take place. These ions are pulled away from the beam before they spread much thermally. This explains the lobe a few centimeters from the exit, close to the beam. Also, the uniform contours above the beam are not what would be expected from thermally spreading ions. The effects of back pressure on the magnitude and location of the charge exchange ions are significant. Their density is lower along the axis without the back pressure, because very few charge exchange reactions take place in the far plume. Also, less charge exchange ions reach the region behind the thruster exit.

The constant velocity case (CV) does not take into consideration the effect of the accelerating grid curvature. As Figure 4 shows, the experiment indicates a peak in flux along the centerline near 15 cm from the exit due to the focusing. In fact, there is a waist found experimentally[4] at this location. To account for the focusing, the dish is assumed to be spherical which, together with the dish depth of 5 mm, specifies the focal point at 25.25 cm from the thruster exit. Use of a spherical velocity profile (SV) in the simulation provides a peak ion flux that is well above that of the experiment, and is therefore not shown in this figure. The location of the peak falls about 5 cm short of the focal point due to deceleration of the beam caused by the grid potential boundary condition. A test case which assumes a parabolic dish gives similar results. Clearly, the paths of the ions are not determined exactly by the dish geometry.

The focusing of the grid is much less pronounced than a fully spherical grid predicts as shown in Figure 5. The true profile must lie somewhere between this and a constant velocity profile which provides no focusing. To help quantify the departure from full focusing, the spherical and constant velocity profiles are superimposed. Mixed profiles of 5% spherical, 95% constant velocity and 10% spherical, 90% constant velocity are each employed. The 5% case agrees well with the magnitude of the experimental flux (see Figure 6), but it too has a very pronounced peak. Figure 6 also shows that the constant velocity case agrees well in shape with the experiment. Figure 7 shows good agreement for all cases with the

experiment 5 cm axially from the thruster exit.

Comparisons of potential along the axis between the cases considered and de Boer's data are shown in Figure 8. Except for the fully spherical profile (SV), all cases shown compare reasonably well with the experiment. As with ion flux, the constant velocity case (CV) shows a gradual decline in potential. The difference in peaks in potential between the fully spherical case and the experiment reflects the magnitude of the discrepancies in ion density. The simulation results are averaged over 1,000 time steps to give time averaged results. In the actual simulations these values vary each time step. The magnitude of these variations could be reduced by employing more ion particles per cell. The number of ions in the simulation is only about 13,000 because the neutral density is much higher (a factor of 80) at the thruster exit. To allow more ions without inordinate memory and computational requirements, a particle weighting scheme is to be added to the code.

Pollard measured ion density in the plume at various angles at fixed distances from the exit using a Langmuir probe for a slightly higher thrust (20 mN).[5] Comparisons of ion density at 30 cm from the thruster exit between the constant velocity simulations and this data are presented in Figure 9. Results obtained with values for T_e of 1 and 5 eV are shown. Qualitatively, the simulation results agree quite well with the measured data.

Figures 10 and 11 show comparisons at 61 cm and 122 cm from the exit. In each case, the constant velocity profiles over predict the ion density at the axis. The lower peak in the experiment could be affected by the focusing of the beam, since these measurements are after the focal point. Consistent with these peaks, the experiment shows more spreading at large angles away from the axis. The spherical profile cases agrees well in shape away from the exit plane, but again the ions are too concentrated near the centerline. In general, these results illustrate the sensitivity of the computed flow field to the initial profile assumed at the exit plane.

Conclusion

A hybrid direct simulation Monte Carlo, Particle-in-Cell code has been developed for computation of plumes from ion thrusters and stationary plasma thrusters. It is capable of calculating both charge exchange and momentum transfer collisions between neutrals and ions. It allows specification of a back pressure for simulation of laboratory experiments. Electrostatic effects can be included or ignored without altering the code. The implicit grid scheme permits a large number of PIC grid cells without sacrificing memory. Two separate grids can be maintained independently. The two particle methods can be maintained independently allowing modification of one without interfering with the other.

The new code was applied to simulate the plume from the UK-10 ion thruster. The expected ion dynamics were captured qualitatively. The beam ions spread more than they would due to purely thermal effects. The charge exchange ions are pulled back towards the thruster near the exit and away from the beam further away.

The simulation results compared satisfactorily with available experimental data for ion flux, ion density, and floating potential. These comparisons also indicated the significance of the initial ion velocity profile assumed in the computations. The cases where spherical grid effects were included indicated that the ion beam, although altered noticeably, followed its initial profile in the near plume. The constant velocity cases at different electron temperatures showed very little variation in this region. A better understanding of the trajectory of the ions between the screen grids is needed to determine the profile at the thruster exit more accurately.

Acknowledgments

Funding for this research was provided by NASA Lewis Research Center through grant NAG3-1451 with Eric Pencil as grant monitor.

References

[1] G.A. Bird, *Molecular Gas Dynamics and the Direct Simulation of Gas Flows*, Oxford University Press, 1994.

[2] C.K. Birdsall and A.B. Langdon, *Plasma Physics Via Computer Simulation*, Adam Hilger, 1991.

[3] D.G. Fearn, A.R. Martin, and P. Smith, "Ion Propulsion Research and Development in the UK," *Journal of British Interplanetary Society*, Vol. 43, No. 10, 1990.

[4] P.C.T. de Boer, "Electric Probe Measurements in the Plume of an Ion Thruster," *Journal of Propulsion and Power*, Vol. 12, No. 1, Jan.-Feb. 1996, pp. 95-104.

[5] J.E. Pollard, "Plume Angular, Energy, and Mass Spectral Measurements with the T5 ion Engine," AIAA Paper 95-2920, July 1995.

[6] D. Rapp and W.E. Francis, "Charge Exchange Between Gaseous Ions and Atoms," *Journal of Chemical Physics*, Vol. 37, No. 11, 1962, pp. 2631-2645.

[7] R. Samanta Roy, "Numerical Simulation of Ion Thruster Plume Backflow for Spacecraft Contamination Assessment," Ph. D. thesis, MIT, 1995.

[8] I.D. Boyd, D.B. VanGilder, and X. Liu, "Monte Carlo Simulation of Neutral Xenon Flows of Electric Propulsion Devices," IEPC Paper 97-20, August 1997.

[9] W.M. Ruyten, "Density-Conserving Shape Factors for Particle Simulations in Cylindrical and Spherical Coordinates," *Journal of Computational Physics*, Vol. 105, 1993, pp. 224-232.

[10] S. Dietrich and I.D. Boyd, "Scalar and Parallel Optimized Implementation of the Direct Simulation Monte Carlo Method," *Journal of Computational Physics*, Vol. 126, 1996, pp. 228-243.

[11] J. Wang, J. Brophy, and D. Brinza, "3-D Simulations of NSTAR Ion Thruster Plasma Environment," AIAA Paper 96-3202, July 1996.

[12] R.M. Myers, E.J. Pencil, V.K. Rawlin, M. Kussmaul, and K. Oden, "NSTAR Ion Thruster Plume Impacts Assessments," AIAA Paper 95-2825, July 1995.

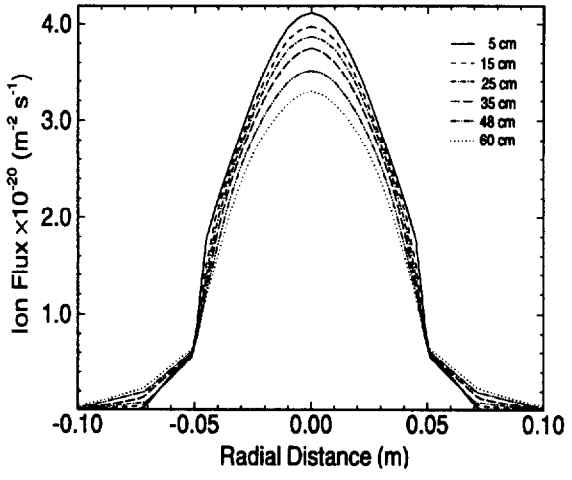

Figure 1: **Radial profiles of ion flux at various axial locations for $T_e = 1eV$.**

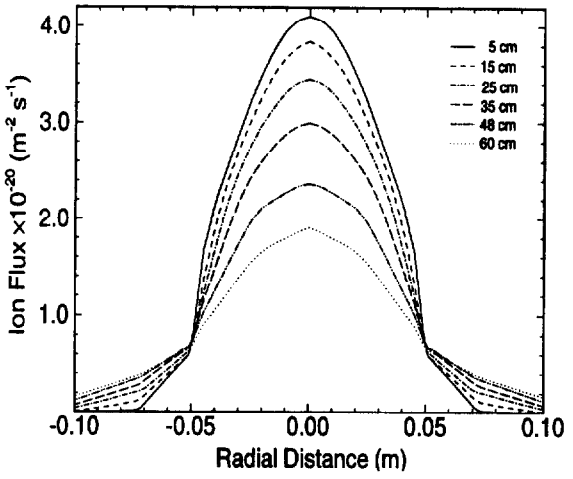

Figure 2: **Radial profiles of ion flux at various axial locations for $T_e = 5eV$.**

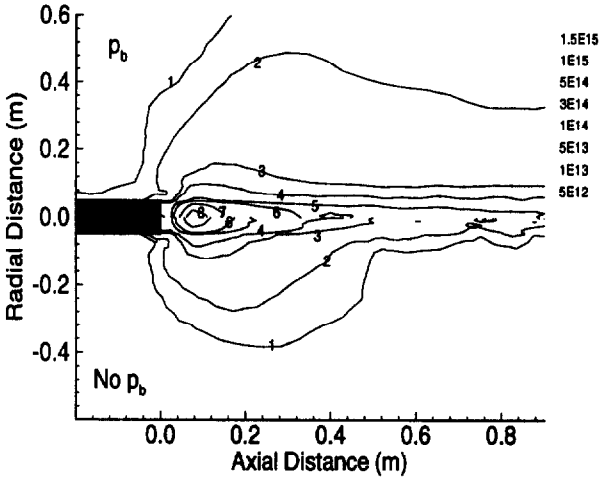

Figure 3: **Contours of CEX Ions for constant velocity case with and without back pressure.**

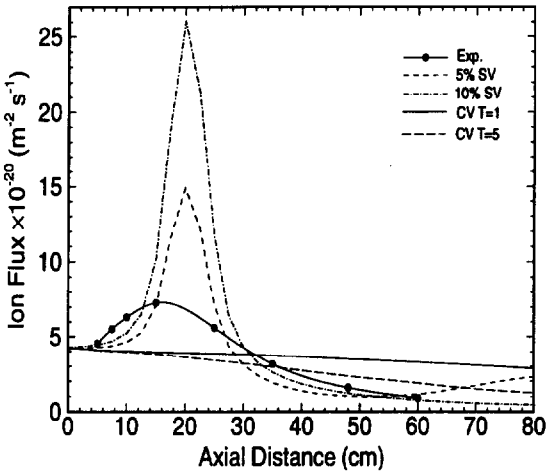

Figure 4: **Comparisons of ion flux along the axis for various cases with experimental measurements by de Boer.**

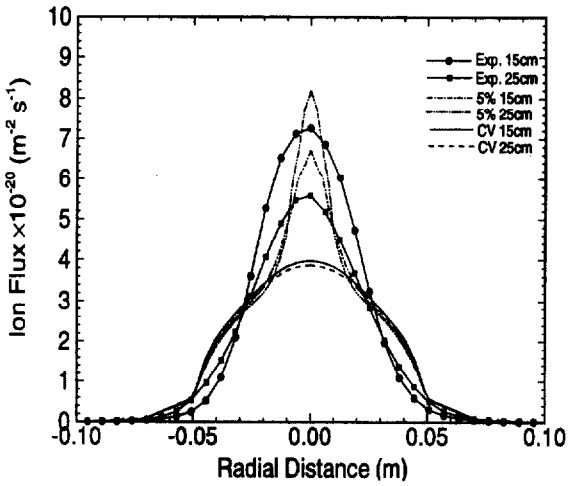

Figure 6: **Comparisons of ion flux from various test cases to experiment at 15 cm and 25 cm from the exit.**

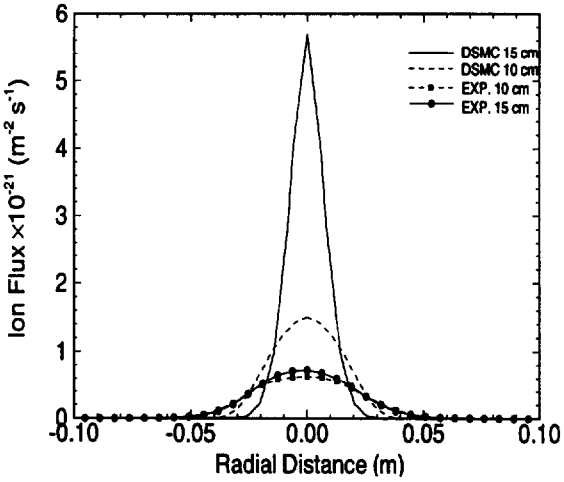

Figure 5: **Comparisons of spherical test case with ion flux from experiment.**

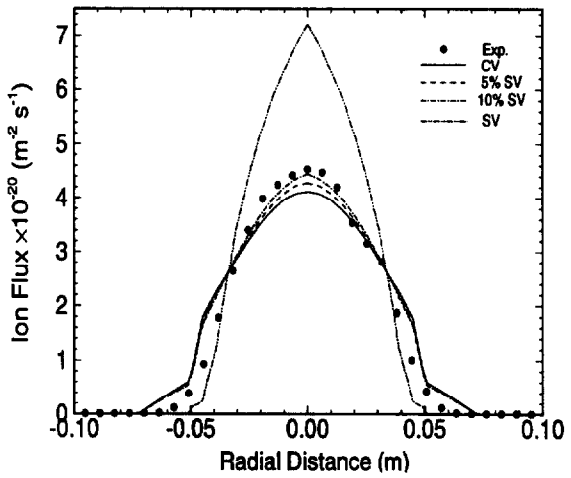

Figure 7: **Comparisons of ion flux from various test cases to experiment at 5 cm from the exit.**

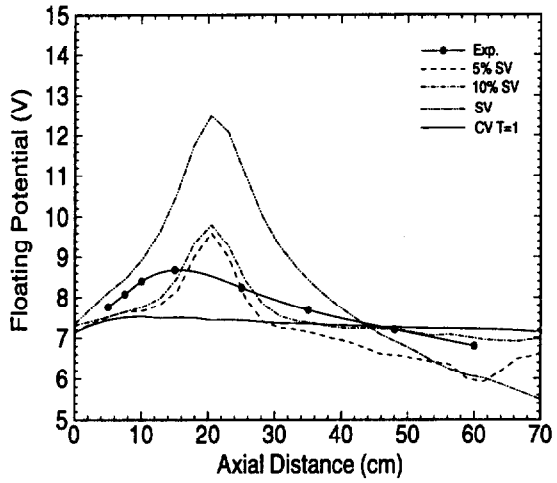

Figure 8: **Comparisons of floating potential along axis for various cases.**

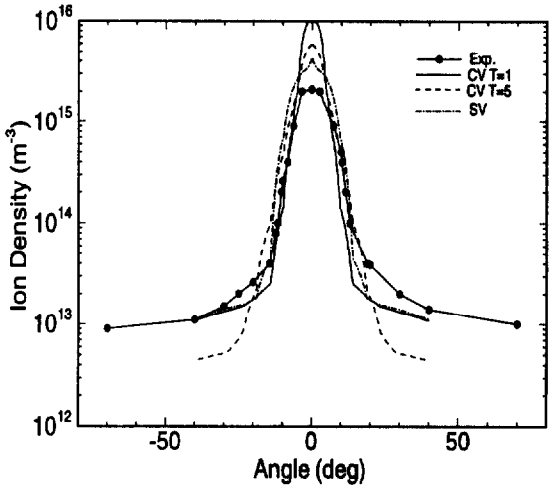

Figure 10: **Comparisons of ion density to experimental measurements taken at various angles 61 cm from the center of the exit.**

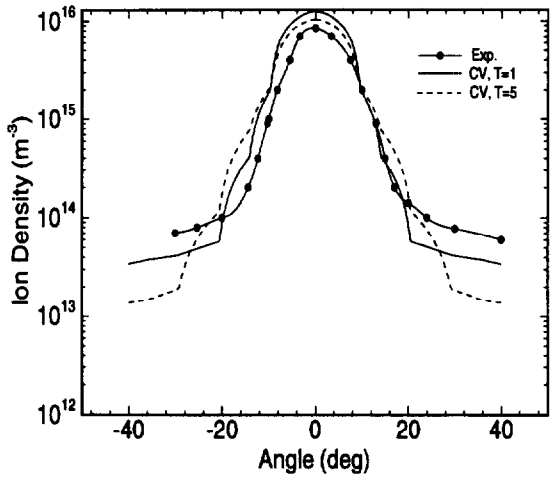

Figure 9: **Comparisons of ion density to experimental measurements by Pollard taken at various angles 30 cm from the center of the exit.**

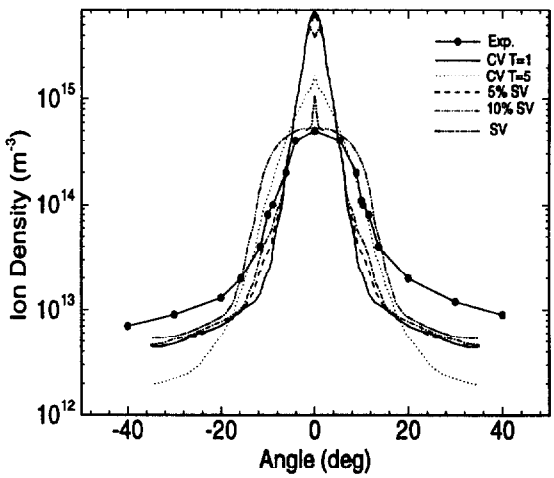

Figure 11: **Comparisons of ion density to experimental measurements taken at various angles 122 cm from the center of the exit.**